Impact of in-situ gas liberation for enhanced oil recovery and CO 2 storage in liquid-rich shale reservoirs

Pedram Mahzari, Adrian P Jones, Eric H Oelkers

Impact of in-situ gas liberation for enhanced oil recovery and CO_2 storage in liquid-rich shale reservoirs

Pedram Mahzari, Adrian P. Jones, Eric H. Oelkers
Department of Earth Sciences, University College London

Abstract

Carbon dioxide injection in shale reservoirs can be beneficial for enhanced oil recovery and CO_2 storage scenarios. CO_2 mass transfer can be influenced strongly by the in-situ liberation of light oil components from live oil forming a distinct gas phase. This mechanism has been overlooked in the past for studying CO_2 and oil interactions in tight formations. In this work, a series of analytical solutions and numerical simulations were developed to identify the effect on EOR by CO_2 due to the liberation of a light hydrocarbon gas phase from live oil in shales. The analytical model demonstrated faster diffusion of CO_2 in the two-phase system due to the presence of this gas phase. Using numerical approaches, laboratory-scale simulations indicated that in-situ gas formation can increase oil recovery by 35%. At the field-scale, an additional oil recovery of 9.8% could be attained. Also, the CO_2 storage capacity of shale formations could be significantly enhanced due to capillary trapping of CO_2 in the liberated gas. The results of this study could potentially be used to improve evaluations of the potential of CO_2 EOR in shale reservoirs.

Keywords: Enhanced oil recovery, CO_2 storage, Shale oil, CO_2 injection, Huff-n-puff , Phase behaviour, Simulation, Unconventionals

1. Introduction

Gas injection for purpose of enhanced oil recovery (EOR) in unconventional liquid-rich reservoirs such as shale oils has become the next frontier for exploitation of shale oil resources [1-7]. EOR for tight oils has both economic and environmental benefits. Increasing oil recovery would improve the net present value (NPV) of a field, which would make it more profitable to operate[7]. Amongst proposed EOR methods, gas based injection scenarios have been recognized as viable methods since gas transport can be more achievable compared to liquids due to favorable viscosity of gases[2,8,9]. Improving oil recovery from tight formations would reduce the need for re-fracking, which alleviates some environmental concerns. CO_2 injection into unconventional reservoirs leads to oil swelling and hence, additional oil recovery[10-13]. Concurrently, CO_2 sequestration in underground geological formations has become one of the viable approaches for attenuating carbon emissions[14-16]. The injection of CO_2 into shale oil reservoirs is an attractive method for the subsurface storage of CO_2[17,18]. The pore scale mechanisms controlling the CO_2 transport, however, are not well understood. In this work, we illuminate a newly recognized mechanism for CO_2 EOR and CO_2 storage based on CO_2 diffusion into the oil leading to the release of a light hydrocarbon gas from the oil phase[19,20]. This process can (i) significantly improve the performance of

EOR in fractured shales, (ii) increase significantly CO_2 storage capacity, and (iii) reduce environmental impacts of CO_2 injection in shales.

Conventional production from shale oil reservoirs requires drilling a large number of wells, and then stimulating them by extended and multi-stage fracking[21]. The average life span of such producing wells is short and hence, these wells are frequently re-fracked, which introduces higher levels of environmental risk[22]. EOR in tight oils can improve the output of producing wells reducing the need for re-fracking. Our analysis indicates that an efficient CO_2 EOR would increase the oil recovery by 10%, which can be a reasonable replacement for re-fracking. This study is aimed at improving our ability to quantify the physics and processes taking place during EOR in unconventional reservoirs.

Previous studies of CO_2 injection in shale oil systems considered reduced conditions where the oleic phase did not contain dissolved gases, which is called dead crude oils[23-25]. Dead crude oil models do not capture the mechanism of gas liberation from 'live oils'. In other words, lack of comprehensive studies of the role of light hydrocarbons in CO_2 EOR has led to over simplifications in the laboratory and numerical simulation of the EOR in shale oil reservoir where the oil used in the shale rock was depleted from its light hydrocarbons[26,27].Therefore, laboratory experiments do not generally report in-situ gas liberation rates[28,29], which would lead to significant under-estimation of oil recovery potential and CO_2 storage capacity of shale oil reservoirs[28,30]. A few reports, however, have focused on in-situ gas formation from 'live oils' during huff-n-puff processes, where in-situ gas expansion could be the dominant pore-scale mechanism expelling oil out of the matrices[31]. In other words, the novelty of this work is to highlight the crucial role of using representative fluid parameters (i.e. live oils) for processes under CO_2 diffusive flow such as CO_2 huff-n-puff in shale oil reservoirs.

In addition, numerous numerical and simulation studies have been performed on the interactions between CO_2 and shale oil formations during huff-n-puff scenarios[4,10,18,32,33]. The fluid model used in these past studies do not capture the mechanism of in-situ gas liberation[34,35]. To capture this mechanism, the compositional model needs to be adjusted to best describe CO_2-oil interactions (binary interaction parameters should be tuned). Specifically, when the model is not equipped with modified binary interaction coefficients, the simulation cannot capture this mechanism. In previous numerical studies, the fluid model could not capture "liberation of light hydrocarbons" as CO_2 diffuses into the liquid-rich shales[4]. To be able to capture this mechanism, which is different from vaporization process, binary interaction coefficient between CO_2 and other hydrocarbon components should be tuned in a way that, diffusion of CO_2 would expel (*not* vaporize) methane, ethane, and propane from the live oil solution[36]. Fundamentally, the conventional CO_2 flooding would cause a condensing-vaporising mechanism for oil-CO_2 interactions[37], whereas, CO_2 diffusion from fracture into the matrix saturated with oil is dominant in

liquid-rich shales. The difference in mass transfer regime between conventional CO_2 flooding and CO_2 diffusive transport in tight reservoirs would necessitate new approach for evaluation of CO_2 EOR in liquid-rich shales[38,39]. In this study, with aid of a fluid model tuned for CO_2 diffusion occurring in a similar process, the impact of gas liberation was studied[40,41]. Therefore, this work aims to demonstrates the role of light hydrocarbon interactions with CO_2 under diffusive mass transfer in fractured tight reservoirs, which was overlooked in previous laboratory and modelling studies.

In addition to the having an impact on EOR, the liberation of light hydrocarbons from the 'live oil' could increase the CO_2 storage capacity by 30% due to CO_2 transfer into the liberated gas phase coupled to its capillary trapping. In this work, the significance of this gas-liberation mechanism is studied using a series of numerical and conceptual models. The purpose of this contribution is to report the results of these models illuminating the consequences of the evolution of this liberated light hydrocarbon phase on CO_2 EOR and subsurface CO_2 storage.

2. Theoretical background

Based on analogous physical processes, in-situ gas liberation takes place during CO_2 diffusion into shale oil matrices[41,42]. Figure 1 illustrates schematically the difference of CO_2 transport between conventional and unconventional (e.g. shale oil) reservoirs. For conventional CO_2 flooding, where gaseous CO_2 is in direct contact with the resident oil in the pores, condensing and vaporising mechanisms would be in play[37,43,44]. When a direct interface between CO_2 and oil exist, interfacial mass transfer would dominate the displacement efficiencies as described by miscibility development paths[45]. However, for the processes under CO_2 diffusive mass transfer into the oil such as carbonated water injection[42] and CO_2 transfer to bypassed oil[46,47], the existence of a clear interface between gaseous CO_2 and the oil is not conceivable. CO_2 and gas injection scenarios for liquid-rich shales are significantly influenced by diffusive mass transfer into the shale oil matrices[48-50]. In shale oil reservoirs, once CO_2 is injected into a fracture, the diffusion of CO_2 through the oil makes the oil act as a membrane, allowing CO_2 to penetrate into the matrix. The oil away from the fracture interacts with the diffused CO_2 unlike in conventional oil reservoirs, where CO_2 is in direct contact with the oil in the invaded pores[4].

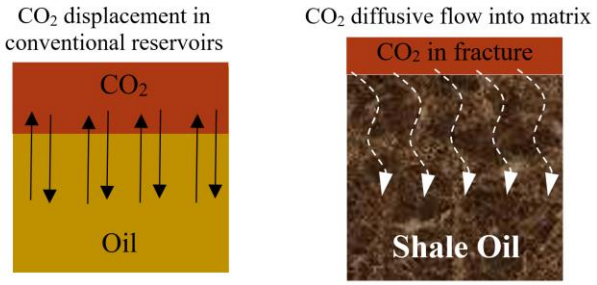

Figure 1: Schematic illustration of the fundamental differences between conventional CO_2 displacement (left side) and CO_2 diffusion into shale oil matrices (right side). In conventional CO_2 displacement, gaseous CO_2 is in direct contact with the oil

leading to mass transfer. In the CO_2 diffusion into shale oil, the oil away from the fracture is not in direct contact with the CO_2 stream.

This diffusive mass transfer of CO_2 into the matrices is analogous to processes taking place during carbonated water injection or CO_2 diffusion into water-shielded oil, where CO_2 is transferred from the injected water into the resident oil[52]. In live oils with significant amounts of dissolved gas, the CO_2 mass transfer liberates light hydrocarbon components as a gaseous phase. Figure 2 illustrates the formation and growth of this gas phase during carbonated water injection as reported by Seyyedi et al[52]. A light oil (a mixture of a crude oil with decane) was injected into a glass microfluidic model to saturate the pore spaces. As can be seen in Figure 2, an isolated oil ganglion (resembling oil in the shale oil matrix) has interacted with flowing carbonated water (resembling CO_2 in the fracture) resulting in the CO_2 transfer towards the oil ganglion. This leads to significant light hydrocarbon gas liberation within the oil ganglion and hence, considerable swelling of the hydrocarbon phase. The key factor controlling this process is the dissolved light to intermediate hydrocarbon composition of the live oil. The liberated light hydrocarbons gas phase leads to swelling because this gas phase remains immobile. This swelling boosts the energies controlling the oil production. This process has generally been overlooked in the past and, as such, the efficiency of CO_2 EOR and CO_2 storage in tight formations has been underestimated.

Another implication of light hydrocarbon gas liberation is the additional capacity for CO_2 storage in shale oils. A substantial portion of the in-situ liberated gas phase would be composed of CO_2 (up to over 80%[41]). Also, it has been demonstrated that this in-situ gas phase would be immobile until it grows beyond 15% gas saturation[42]. These two factors (i.e. high CO_2 concentration in gas phase and highly immobile gas saturation) would lead to the capillary trapping of some of the injected CO_2. Therefore, not only significant additional oil recovery can be achieved, also notable amount of CO_2 storage can be attained.

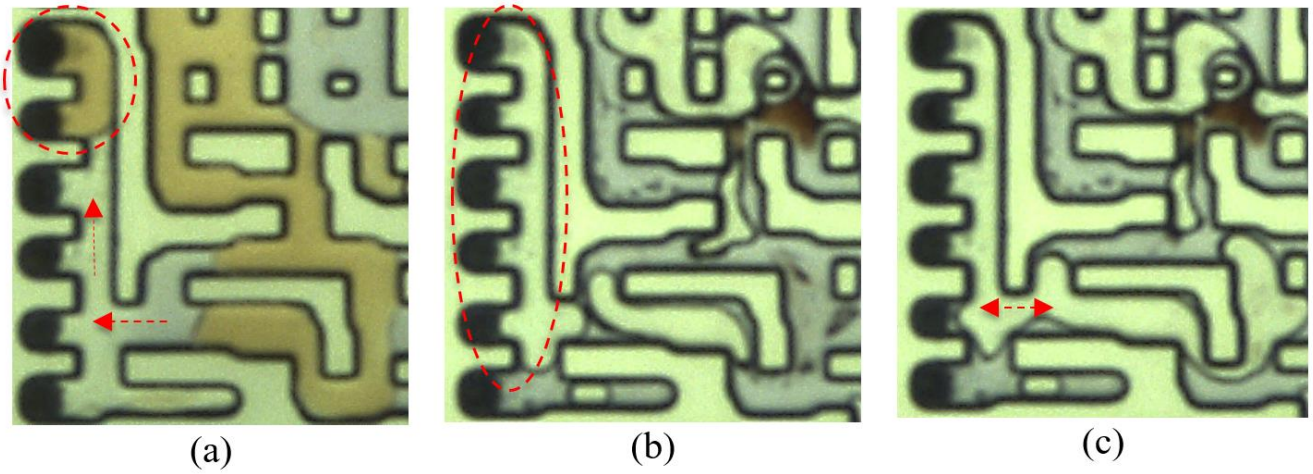

Figure 2: A sequence of pore-scale observations of in-situ gas phase formation during carbonated water injection. The liquid oil in image (a) is brownish and trapped in a dead end pore. The carbonated water flowing in the neighbouring flow paths has blue colour due to blue dye. The red arrows on (a) indicate the CO_2 diffusion path towards the isolated ganglion. From (a) to (c), the isolated brownish oil converts to a white gas phase as highlighted by dashed red circle. The diffusion of CO_2 from carbonated water into the isolated oil leads to hydrocarbon expansion of approximately 300%. This expansion factor was

estimated from the image analysis of theoil ganglion. Based on (c), as highlighted by a red arrow, this expansion resulted in the re-joining of the isolated ganglion with other pores. The micromodel images are taken from the experimental investigation performed by Seyyedi et al.[52].

Having illustrated the gas liberation mechanism during carbonated Water injection,

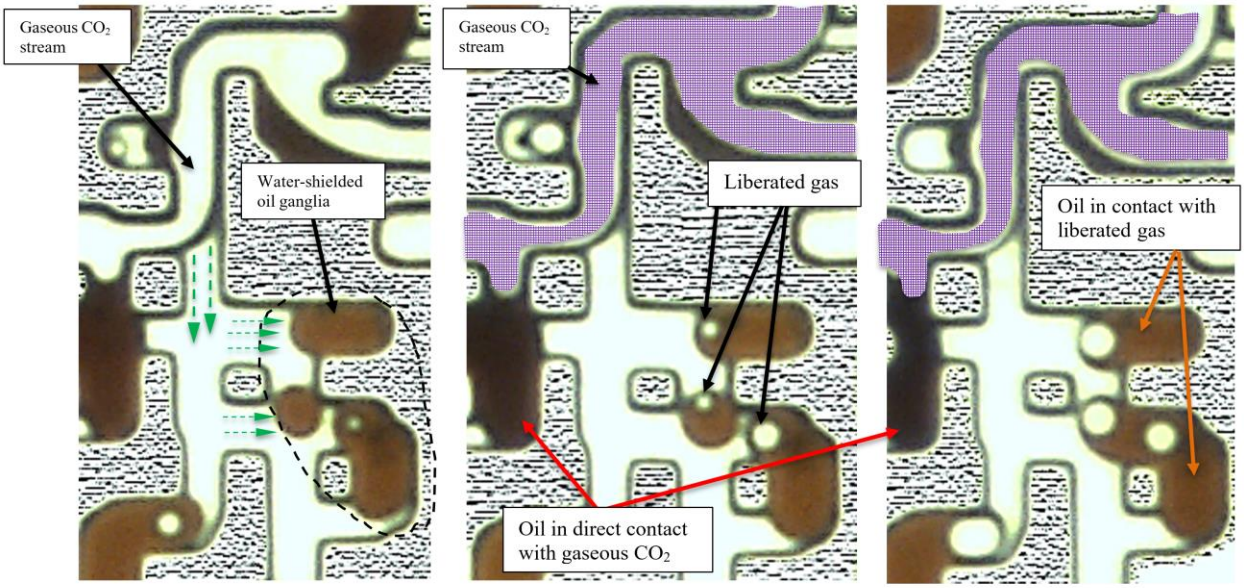

Figure 3 shows a series of images taken from dry CO_2 injection in glass micromodel using a live crude oil[51]. In

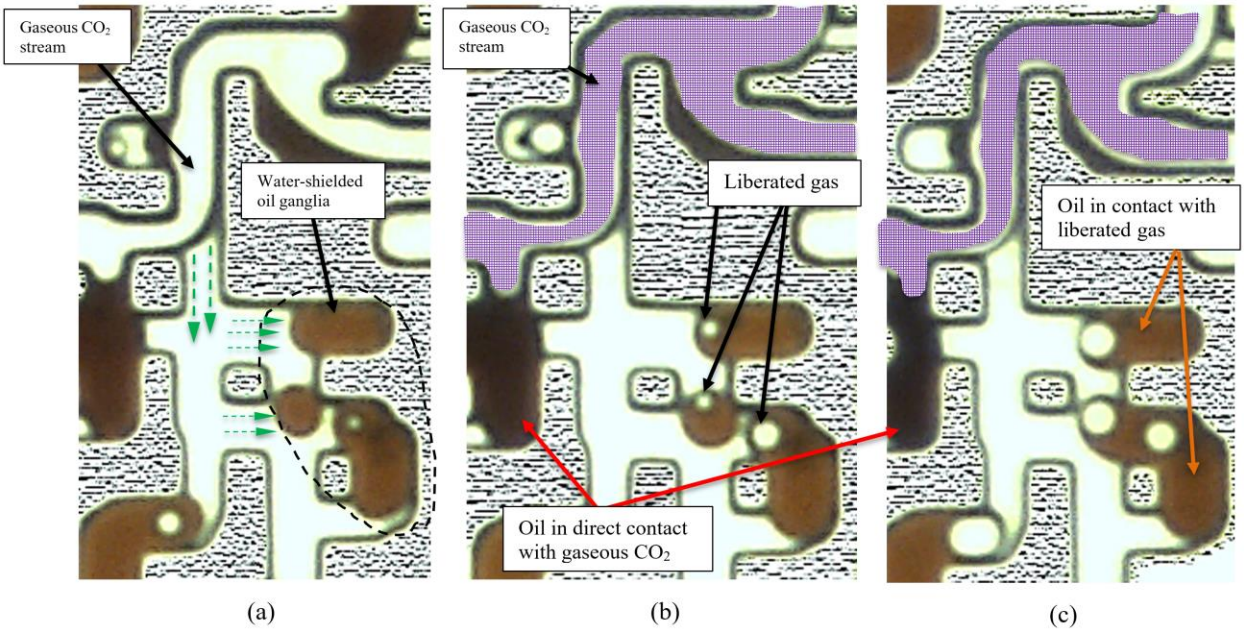

Figure 3a, two different oil ganglia can be identified under different interactions, i.e. direct and diffusive interactions with CO_2. Comparison of

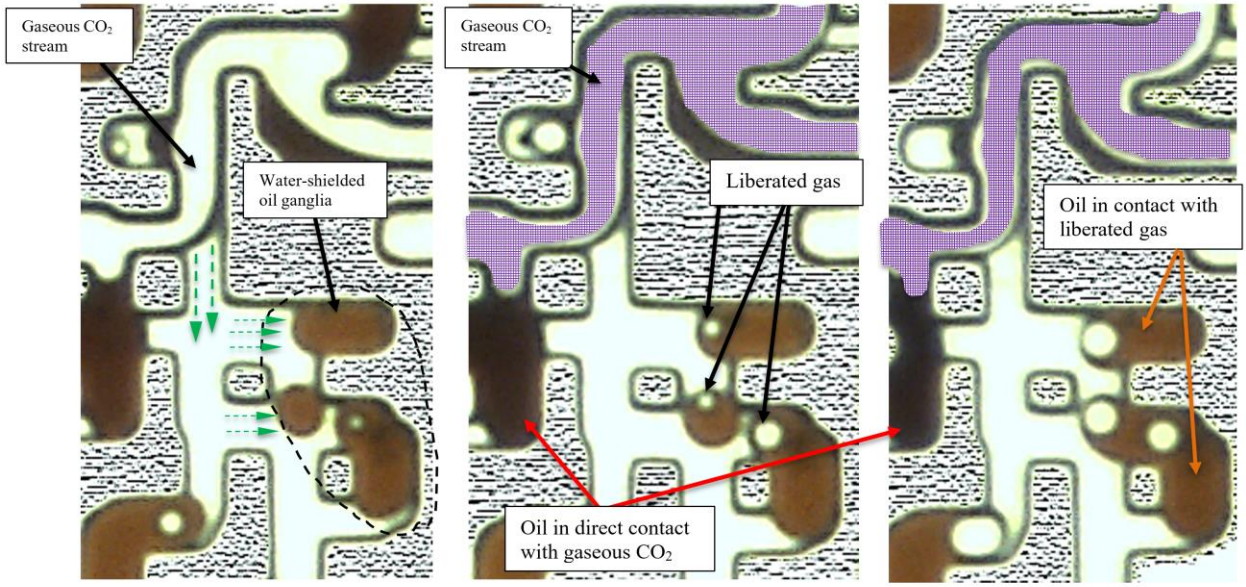

Figure 3b and c indicates that the oil under vaporisation (i.e. the dark oil under direct contact with the CO_2 stream) can exhibit different behaviour compared to the oil under diffusion of CO_2 (i.e. brownish oil showing gas liberation mechanism). As reported by[36,53], equation of state parameters for these two interactions are not similar. The CO_2 diffusive mass transfer would be predominant in shale oil reservoirs[48]. However, previous studies for CO_2 interactions in shale oils have considered phase behaviour pertinent to direct contact between CO_2 and oil[4,10,33,35,54,55]. Therefore, it appears that, a comprehensive analysis of CO_2 diffusive mass transfer in shale oil is needed to highlight the role of gas liberation mechanism during diffusion of CO_2 in shale oil. The novelty of this work is to use a phase behaviour that is tuned for diffusive mass transfer of CO_2 rather than the direct contact of CO_2 and oil.

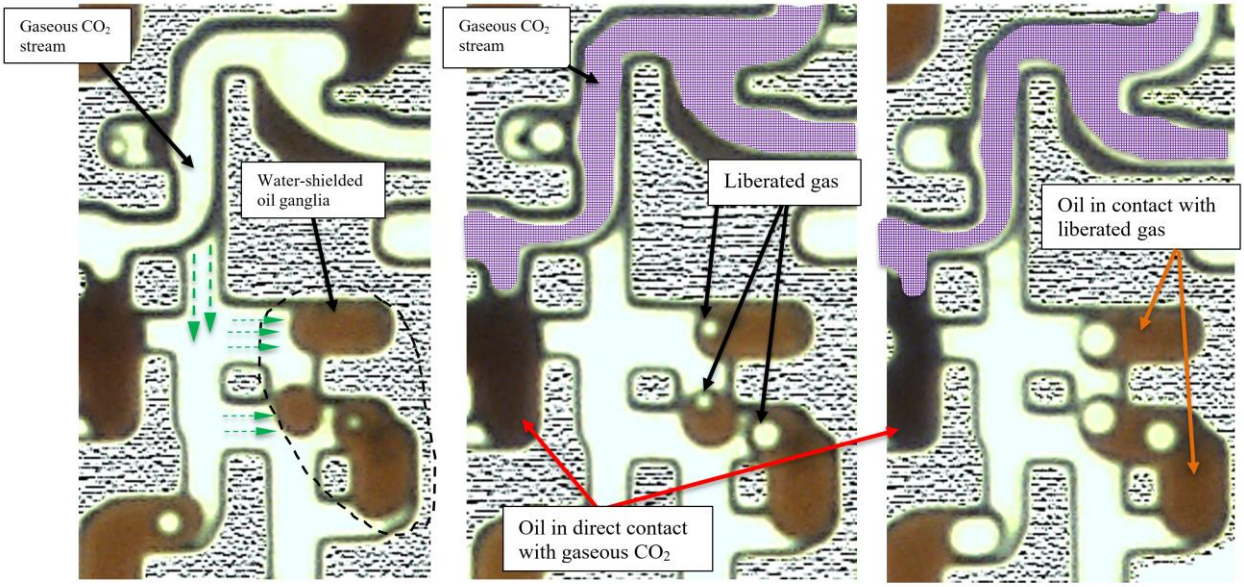

Figure 3: A sequence of pore-scale observations of oil and CO_2 interactions during dry CO_2 injection. Image (a) is a magnified section of glass micromodel under CO_2 injection. In image (b), as CO_2 injection continues, the oil ganglia away from CO_2 stream have started to liberate their gas content. The gaseous CO_2 stream is digitally coloured purple. Image (c) illustrates the magnified snapshot of the micromodel after extensive injection CO_2. Comparison of image (b) and (c) demonstrates that the oil in direct contact with CO_2 stream is significantly darker than the oil under diffusive CO_2 mass transfer. This highlights the fact that gas liberation mechanism (taking place for the oil under diffusive CO_2 mass transfer) can bring about different phase behaviour compared to vaporisation mechanism (occurring for the oils under direct contact of CO_2 stream). The micromodel experiments were performed elsewhere and images have been taken from Seyyedi et al[51].

3. Methodology

Conventional equation-of-state (EOS) parameters are not able to capture gas liberation mechanism. To accurately model this process, therefore, a more representative set of EOS parameters is required. In the present study, a fluid model was first tuned to accurately describe the CO_2 diffusion from an aqueous phase into the resident oil[53]. This model was then upgraded with observations of two core-scale injections of carbonated water injection in tertiary and secondary modes using a co-history-matching approach[56]. This effort leads to EOS and diffusion coefficients that can be employed for the accurate evaluation of the in-situ gas liberation in the liquid-rich shale reservoirs. The parameters controlling the gas liberation and the consequences of this mechanism are binary interaction coefficients between CO_2 and individual oil components[57,58]. Table 1 lists the main EOS parameters used to describe the live oil. Table 2 shows the binary interaction coefficients used for the Peng Robinson EOS[59,60]. As can be seen in Table 2, some of binary interaction coefficients have negative values indicating that the coefficients would lead to liberation of the hydrocarbon components. The EOS parameters presented in Table 1 and Table 2 were obtained by co-history-matching where two coreflood experiments performed on secondary and tertiary carbonated water injection were matched simultaneously. Matching two coreflood experiments together leads to representative EOS parameters, which captures different mass transfer of CO_2 in the live oil. It should be

reiterated that, this work focusses on the mass transfer into shale oil matrices, which is analogous to CO_2 transfer in carbonated water injection.

This study is focussed on the gas liberation in the oil rich matrices, which can be a predominant oil recovery mechanism[20]. However, other pore scale processes can affect the efficiency of CO_2 EOR scenarios in ultra-tight rocks[54]. The diffusion of CO_2 into liquid-rich shales would trigger processes such as asphaltene precipitation[61-63], nano-pore capillary confinement and condensations[64-66], relative adsorption of different components in kerogen and clay rich formations[67], and geomechanical effects[55]. These processes would not be considered in the analytical and numerical evaluations performed in this work. It should be pointed out that, accounting rigorously for in-situ gas liberation would lead to substantial impact on other processes. For example, in the next section, we show that in-situ liberation of gas phase results in significantly higher pressure generated within the matrix, which can cause notable change in geomechanical processes. Therefore, this work can provide insights in improved estimation of other processes during CO_2 EOR in tight reservoirs.

Table 1: EOS parameters for the live oil components.

Component	Pc (atm)	Tc (^oK)	Acentric factor
CO_2	72.8	304.2	0.225
CH_4	45.4	190.6	0.008
C2HtoC3H	45.36	335.76	0.121
IC4toC7	34.20	481.01	0.421
C8 toC9	28.04	584.29	0.371
C10-C15	25.01	664.10	0.639
C16-C20	19.99	730.98	0.774
C21-C25	19	778.52	0.8
C26-C31	18	800.00	0.8
C32-C33	17	800	0.8
C34+	15.99	799.99	0.8

Table 2: Binary interaction coefficients between CO_2 and oil components that could capture the triggering and extent of gas liberation mechanism.

Components	C1	C2toC3	C4toC7	C8toC9	C10toC15	C16toC20	C21toC25	C26toC31	C32to C33	C34+
Co-history-matched	-0.04	-0.03	0.61	0.19	-0.89	0.58	0.68	-0.41	-0.54	0.2

The impact of in-situ gas liberation on EOR and carbon storage has been investigated in this study using two main approaches; analytical solutions and numerical simulation. The analytical modelling uses Fick's second law to account for the enhanced diffusion of CO_2 due to in-situ gas liberation. For the numerical simulations, two systems were considered; (i) laboratory-scale simulations of diffusive flow of CO_2 into shale oil core and (ii) large-scale CO_2 huff-n-puff simulations in a hydraulically fractured reservoir. For the simulations, the CMG-GEM (compositional reservoir simulation package) was used. For the laboratory-scale simulation, a shale oil matrix-core, saturated with a live oil is considered with the top face of the core exposed to a fracture. The CO_2 is assumed to be flowing in the fracture and hence, fresh CO_2 is continuously available in the fracture to be diffused into the matrix. The core-scale models are designed such that, CO_2 can "only" invade by diffusion. As CO_2 diffuses into the matrix, the

hydrocarbon phases in matrix swell. The swollen oil within the core can be extracted from the fracture as well. This concept is used for both the analytical solutions and numerical simulations of laboratory-scale analyses to quantify CO_2 diffusion into matrix. To allow their direct comparison, the dimensions of analytical solutions and numerical simulation were kept identical for the laboratory-scale calculations.

3.1. Analytical solutions with Fick's law (Two phase diffusion)

As CO_2 exists in the fractures and the live oil is saturated within the shale matrix, CO_2 penetrates into the oil by diffusive transport, as depicted in Figure 1. Diffusive flow of a component through a liquid phase can be quantified using Fick's second law (Equation 1), which has been widely used in diffusive mass transfer of gas into hydrocarbon oils[68]. The solution of this equation for fixed boundary conditions and a constant diffusion coefficient would result in the error function expression given by Equation 2. The fixed boundary assumption is similar to gas diffusion in heavy oil experiments where swelling and change in boundary conditions can be ignored[69]. The main concept introduced in this analytical solution is the enhanced diffusion of CO_2 due to in-situ gas liberation. The additional diffusion due to gas phase liberation is a function of the relative saturation of gas and oil phases as given by Equation 3. Note the gas and oil saturation sums to unity as expressed by Equation 4. The diffusion coefficient in a porous media needs to be adjusted based on porosity and tortuosity of the medium[70], which would result in Equation 5. The tortuosity of the shale can be estimated using x-ray tomography[71], which implies an average tortuosity of 10[72]. One important aspect of analytical solutions is the relationship between the gas saturation and CO_2 concentration as expressed by Equation 6.

$$\frac{\partial}{\partial x}\left(D_{eff}\frac{\partial C}{\partial x}\right) = \frac{\partial C}{\partial t} \qquad \text{Eq. 1}$$

$$C_t(x,t) = C_{eq}\, erfc\left(\frac{x}{2\sqrt{D_{eff}t}}\right) \qquad \text{Eq. 2}$$

$$D_{eff} = D_{oil} \times S_{oil} + D_{gas} \times S_{gas} \qquad \text{Eq. 3}$$

$$S_{oil} + S_{gas} = 1 \qquad \text{Eq. 4}$$

$$D_{porous} = D_{eff}\frac{\phi}{\tau} \qquad \text{Eq. 5}$$

$$S_{gas} = f\left(C_t(x,t)\right) \qquad \text{Eq.6}$$

where *x* and *t* stand for the distance from the fracture and time. *C* denotes the CO_2 concentration in the medium. D_{eff} refers to the overall CO_2 diffusion coefficient into the hydrocarbon phases. C_{eq} designates

the CO_2 concentration at thermodynamic equilibrium and $C_t(x,t)$ represents the CO_2 concentration due to diffusive flow into the shale. D_{oil} and D_{gas} refer to diffusion coefficients of CO_2 in the distinct oil and gas phases, respectively. S_{oil} and S_{gas} represent the saturations of oil and gas phases in the shale. D_{porous} stands for the effective diffusion coefficient in porous media accounting for both porosity (ϕ) and totuoisity (τ).

Equations 2 to 6 are used to calculate the CO_2 concentration profiles within the oil due to diffusion. The equations are solved with assumption that CO_2 is in thermodynamic equilibrium at the top interface, which represents the fracture as a fixed boundary condition. Since the effective diffusion coefficient depends on the gas saturation (Equation 3), the correlation between CO_2 concentration and gas saturation (Equation 6) plays an important role in the determining concentration profiles. These equations are solved in an iterative mode to obtain CO_2 concertation profiles. The PVT package of the CMG software was used to plot gas saturation versus total CO_2 concentration as illustrated in Figure 4. As shown in Figure 4, to constrain the EOS data, a logarithmic model was used to fit the relationship between gas saturation and CO_2 concentration. Once the required input parameters for the model are identified, Equation 2 is solved iteratively. The model was solved assuming the diffusion coefficient for CO_2 through the gas phase is 10 times higher than that of the oil phase[73].

The analytical solutions require several simplifying assumptions; (i) the diffusion coefficient is constant and independent of pressure, temperature and composition. As the pressure and temperature variations are not high, this assumption is reasonable. However, the effect of composition can impact the results as CO_2 composition can impact the oil viscosity significantly and hence, diffusion coefficient can be impacted[69]. Due to lack of experimental data for oil viscosity variations with respect to CO_2 compsition, this impact was neglected here in the analytical model. (ii) the equations are solved under constant pressure and temperature conditions. Oil swelling and gas liberation would bring about local pressure rise within the pores, which can impact the results, however, to avoid complexity of local pressure variations, the equations were solved under constant pressure. The impact of local pressure variations could be studied in the next section via numerical simulations. (iii) the media acts like a cylinder with fixed boundary conditions (the permeability of the porous media does not affect the concentration profile). This assumption has been reflected in the fact that the problem is pure diffusion and no convection is considered. The impact of porous media is only manifested in equation 5. (iv) the gas phase is immobile. This assumption is fairly valid for gas saturation below 10%[40]. One objective of this analytical solution is to highlight the importance of gas liberation on CO_2 transport within the oil shale matrices. In the subsequent section, the results of high-resolution numerical simulations are compared with analytical solution results to evaluate the significance of model simplifications. The length of the porous media is

25 cm and diameter of the core-scale media is 3.81 cm. A diffusion coefficient of 8×10^{-4} cm^2/s and porosity of 0.08 were used for the analytical solution.

Figure 5 illustrates the CO_2 concentration profiles at different times along the porous media for the laboratory-scale obtained from analytical solutions run with and without gas liberation. The CO_2 concentration for the case with gas liberation has a higher degree of CO_2 penetration over laboratory time scales. For instance, after 20 hours and 5 cm away from the fracture located at the top of the core, the calculated molar concentration of CO_2 is 6% for the no gas liberation case whereas, gas liberation can boost up the CO_2 concentration to up to 18%. This Fickian diffusion calculation indicates, therefore, a significant impact of in-situ gas liberation on CO_2 transport within the shale oil matrices containing live oil. For the analytical solutions, however, it is essential to obtain the relationship between the total CO_2 concentration and liberated gas volume (or its saturation). This requires performing tailored experiments to quantify diffusive mass transfer, where the volume of liberated gas can be measured. For the analysis performed in this study, we used a fluid model tuned on carbonated water injection experiments. For the more realistic shale oil system of CO_2 diffusion, the analytical solutions developed in this study can be improved by taking account of laboratory experiments designed to generate the data required for tuning the phase behaviour.

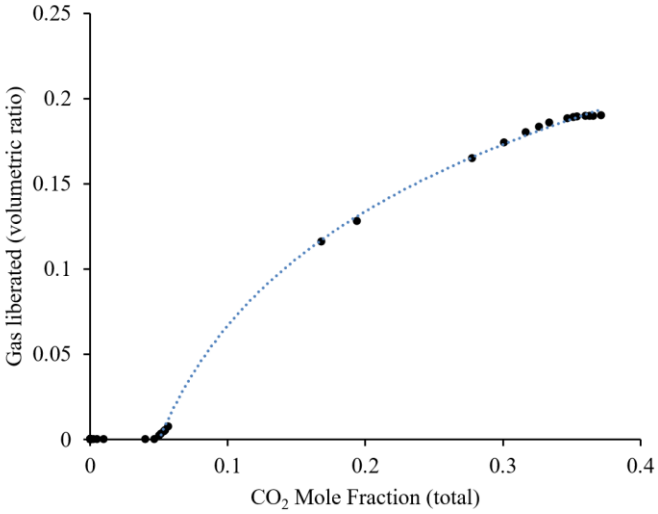

Figure 4: Relationship between gas saturation and total CO_2 concentration as calculated using the EOS tuned for the diffusive CO_2 transfer (black dots). The dotted blue line represents the logrithmic model fit on the gas saturation data obtained from co-history-matching. It should be noted that, the gas saturation was not measured directly in the experiments but, the co-history-matching of two coreflood experiments could enable generating reliable gas saturation data[53].

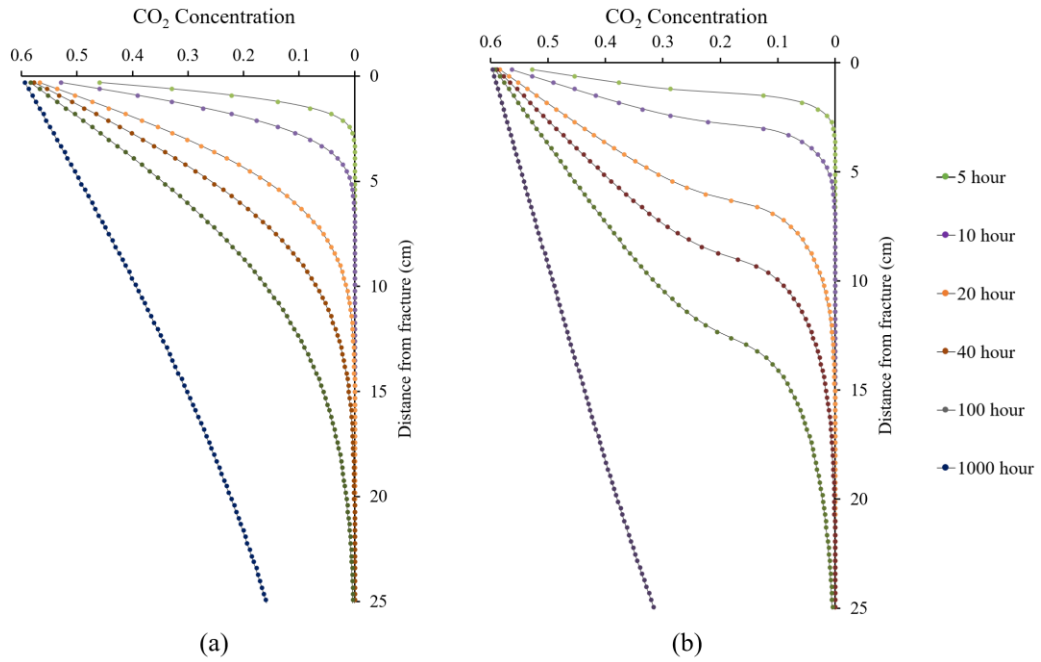

Figure 5: CO_2 concentration profiles estimated using analytical solutions of Fickian diffusion for two cases; (a) no gas liberation and (b) with gas liberation. Gas liberation enhances the CO_2 transport significantly.

The calculation of the CO_2 concentration profiles for the system with and without gas liberation enables calculation of oil recovery for these two cases. For the case where no in-situ gas liberation is considered, the oil recovery is controlled by liquid phase swelling and the CO_2 storage capacity depends primarily on the dissolution capacity of the liquid oil phase. However, when the gas liberation is taken into account, the oil can be driven out by the gas liberation and its expansion in the matrices. The following equation can be used to calculate the oil recovery percent;

$$Oil\ Recovery \quad = S_o(SF(C_{CO2}) - 1) + S_g \qquad \text{Eq. 7}$$

where S_o and S_g refer to the oil and gas saturation, respectively, related via Equation 4. The oil recovery in Equation 7 is calculated as the percent of oil produced under reservoir conditions relative to the original oil in place; no formation volume factor is involved. In Equation 7, *SF* represents the swelling factor of the oil as a function of the CO_2 concentration. Based on the results of EOS calculations, Figure 6 shows the relationship between the CO_2 concentration and the oil swelling factor, which is used for calculating the percent oil recovery in Equation 7. The average CO_2 concentration is calculated from Figure 5 and hence, the corresponding average swelling factor. Thus, in this equation, the swelling factor and gas saturation depends on the CO_2 concentration in the matrix. Based on these assumptions, and using Equation 6 in combination with Figure 4 and Figure 6, the oil recovery for these two cases can be calculated as shown in Figure 7. In-situ gas liberation increases greatly oil recovery. Analytical solutions

indicate that, for live oil with high potential of gas liberation, the additional oil recovery due to light hydrocarbon gas formation can be twice that of the cases when a dead oil phase is assumed.

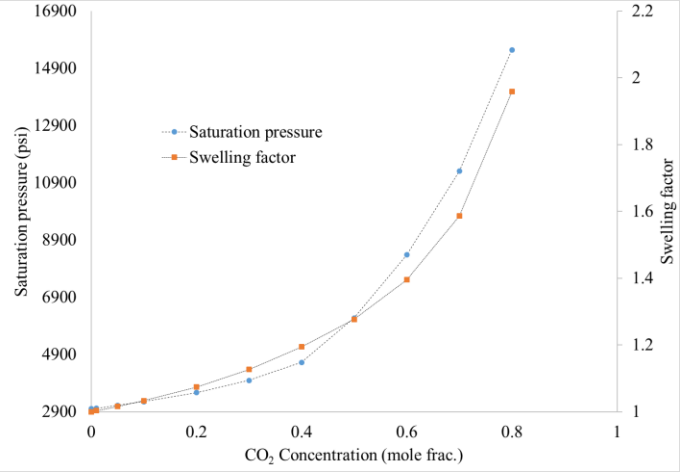

Figure 6: Swelling factor and bubble point pressure (saturation pressure) of the oil with respect to CO_2 concentration in a simulated swelling test. The swelling factor data were used for calculating oil recovery within the analytical solutions. The results of the tuned equation of state indicate an increase in bubble point pressure which is in agreement with in-situ gas liberation, i.e. as CO_2 concentration increases under fixed pressure of 3100 psig, it is expected to have more gas released due to rise in bubble point pressure.

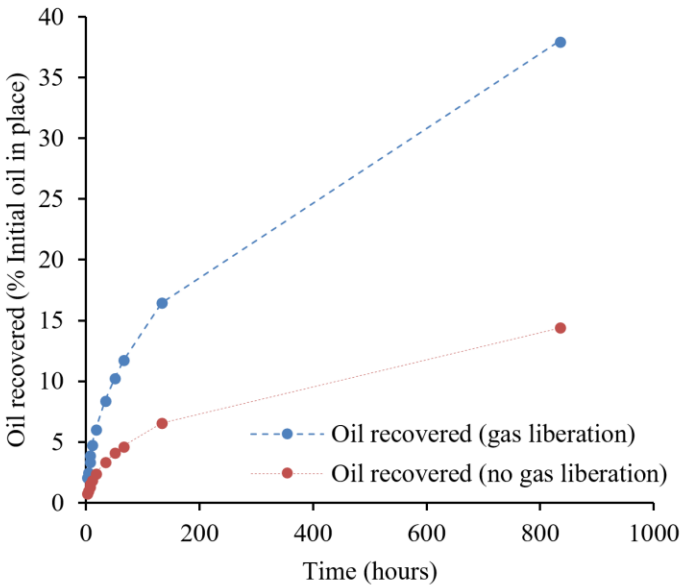

Figure 7: Using equation 7, the oil recovery of the laboratory-scale analytical solutions was calculated for two cases; with and without gas liberation. If the system can generate in-situ gas, the oil recovery is doubled compared to the case when gas liberation was neglected.

3.2. Numerical simulation results

3.2.1. Laboratory-scale simulations

The impact of in-situ gas liberation can be investigated using a high resolution numerical simulations taking into account of the effect of processes such as oil swelling, pressure build up due to swelling, and additional mixing due to gas liberation. In numerical simulations where physical diffusion plays an essential role, numerical dispersion should be minimised. Therefore, the laboratory-scale numerical

simulations with same dimensions as used in the analytical solutions (25 cm length and 3.8 cm diameter) was divided into a 200×200×1000 grid block. Considering the 11 components used (as described in Table 1) in the compositional fluid model, the high-resolution numerical simulations could be computationally costly and hence, the Myriad high performance computing facility at University College London was used. Table 3 shows the input parameters used for the laboratory-scale numerical simulation. The CO_2 was injected through the fracture at a constant injection rate. The production of the oil and gas fluids is controlled to be at constant pressure (i.e. same as initial reservoir pressure) applied on the fracture at the top of the core. As the injection pressure and initial core pressure are equal there is no increase in the pressure due to CO_2 pumping any pressure build-up in the matrix is due to diffusive mass transfer of CO_2 from the fracture to the matrix and consequent hydrocarbon swelling. This initial pressure was chosen to assure that the live oil is above its bubble point and any gas forming within the matrix is associated with the in-situ gas liberation mechanism. Figure 8 illustrates schematically the numerical simulation of the diffusive mass transfer. The results of gas saturation and the pressure profile are plotted for a gird cell located away from the main CO_2 stream in the fracture. The grid cell selected for plotting the results of gird pressure and gas saturation was 5 cm away from the fracture to ensure that, no CO_2 can penetrate into the grid only by diffusion.

Table 3: Input for the numerical simulation

Length (cm)	25
Diameter (cm)	3.81
Matrix Porosity (frac.)	0.08
Fracture Porosity (frac.)	0.01
Matrix Permeability (mD)	0.001
Fracture Permeability (mD)	1000
Core Pressure (psi)	3200
Core Temperature (^oF)	210
Bubble Point pressure (psi)	3100
CO_2 diffusivity in oil (cm^2/s)	8×10^{-4}
CO_2 diffusivity in gas (cm^2/s)	8×10^{-3}
Injection rate of CO_2 through fracture (cc/hr)	0.1

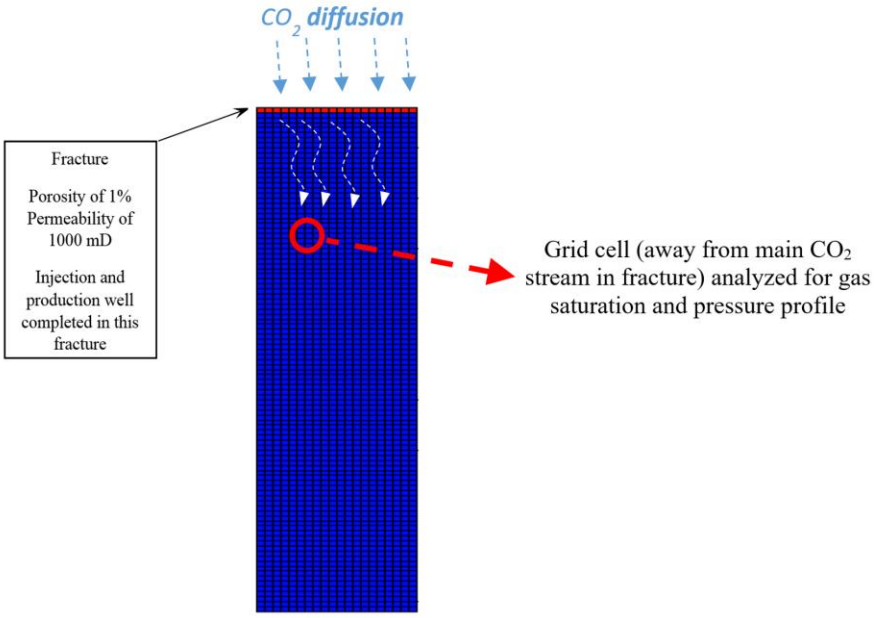

Figure 8: Fracture-matrix configuration in the laboratory-scale numerical simulation created to represent the diffusive-only transport of CO_2 into the shale core saturated with live oil. CO_2 is injected continuously at the top grid cells (in red) and produced from same grid cells. Diffusion of CO_2 in the matrix, 5 cm below the fracture, was considered for analyses of gas saturation and pressure. The boundaries of the matrix (except top boundary) are sealed and hence, oil can only be produced from the top face through the fracture.

Two sets of equation of state (EOS) parameters were used in these laboratory-scale numerical simulations; (a) default values for CO_2 and hydrocarbon components (the default values are between 0.1 and 0.13) and (ii) the tuned values presented in Table 2. The equation of state can capture the gas liberation when a number of binary interaction coefficients are set to negative values as listed in Table 2. Binary interaction coefficients are needed adjusted for unlike components such as CO_2 and hydrocarbon components. Figure 9a shows the pressure and gas saturation profiles in a grid block located 5-cm below the fracture determined from both sets of parameters. Figure 9b depicts the composition of the liberated in-situ gas phase as it grew. The gas saturation (Figure 9a) of the tuned case reached 28% after 30 days, which indicates an acceptable response time compared to normal huff and puff time-scales suggested for shale oils[2,4,10,28,31]. In contrast, using the default values, no gas was formed in the grid block, which demonstrates the importance of using realistic EOS parameters to accurately model the gas liberation mechanism. One consequence of in-situ gas formation is reflected in pressure profiles. As the gas phase formed and evolved, the pressure (or energy) generated in the tuned case (shown by the black curve) is higher than that of the case run using the default values (shown by the yellow curve). This is a consequence of the higher degree of in-situ swelling of hydrocarbons due to in-situ gas formation. This local pressure increase (a 250 psi difference between two cases) can help push the oil towards the fracture. Moreover, the higher pressure may open micro-fractures due to the enhanced local stress imposed on the matrix. It should be noted that the increase in local pressure depends strongly on the matrix permeability; for a

relatively high permeability of 0.01 mD, the incremental pressure difference was 100 psi[19] whereas, for the tighter matrix considered in this study, the incremental pressure difference was 250 psi. This result demonstrates that laboratory experiments for EOR and CO_2 storage should be carried out under full reservoir conditions to accurately reproduce natural systems. Furthermore, as can be seen in Figure 9b, the liberated gas phase is composed of methane primarily at the beginning of the simulation but the CO_2 concentration in the gas phase increases to 70% over time. The temporal composition of the live oil is in agreement with previous laboratory measurements of gas liberation during carbonated water injection[41,53]. Another implication of gas composition evolution is the importance of light hydrocarbons such as methane in the live oil to trigger to the gas liberation.

Figure 10 illustrates the gas phase distribution in the shale core after one day of CO_2 diffusion. The gas forms mostly in vicinity of the fracture (near the top of the core) and advances deeper in the core with time. Note that this gas is immobile, as tuned by co-history matching, for gas saturations below 19%. This gas flow characteristic is consistent with direct observations of this process reported in other studies[40,52]. Figure 11 suggests a 41% oil recovery from the matrix after 30 days of CO_2 diffusion due to the formation of the in-situ gas phase. In the absence of gas liberation oil recovery was 7.1%. The differences in the simulation results are due to in-situ gas formation energizing the matrix, pushing the oil out. The gas composition from fracture to the bottom the system could vary depending on the amount of diffused CO_2. However, the average CO_2 composition of the gas phase was 75% weight percent. Therefore, there is a significant additional CO_2 storage in the form of high pressure immobile gas phase within shale matrices.

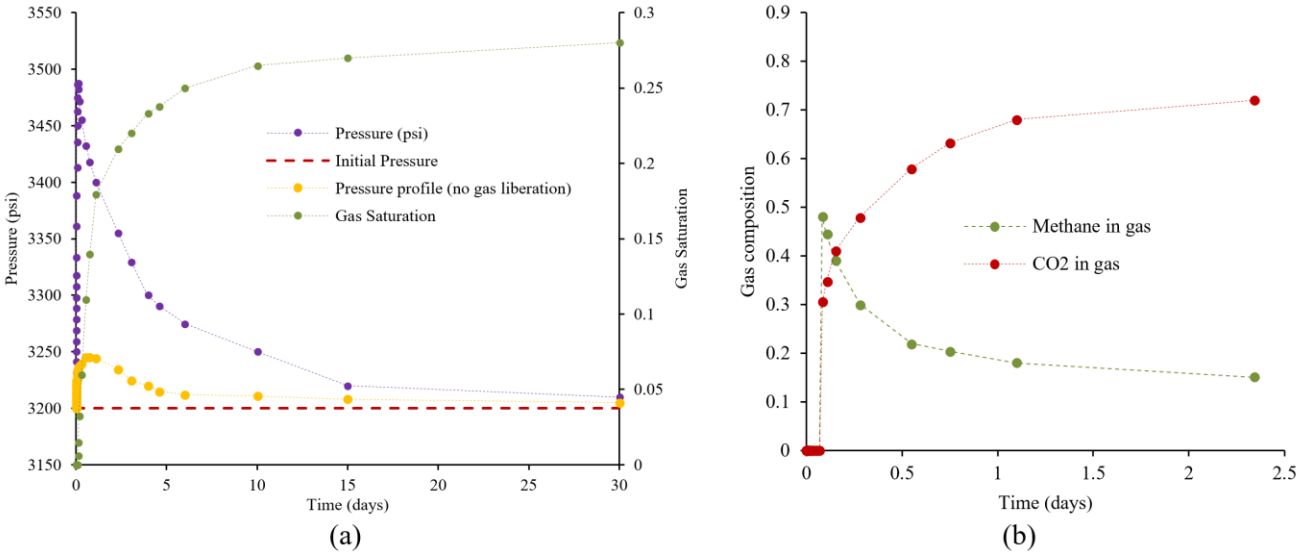

Figure 9: (a) Calculated temporal pressure and gas saturation profiles of the grid block 5-cm away from the fracture for two numerical simulations: one with no gas liberation (yellow curve in (a)), the other having provision for the consequences of the liberation of a light hydrocarbon phase (black curve for pressure and green curve for gas saturation) (b) the gas composition of the grid block 5-cm away from the fracture. From the pressure profiles, the black curve with gas liberation mechanism shows a significantly greater pressure increase due to oil and gas swelling whereas, the yellow curve indicates a limited increase in pressure due to limited swelling of the liquid phase alone.

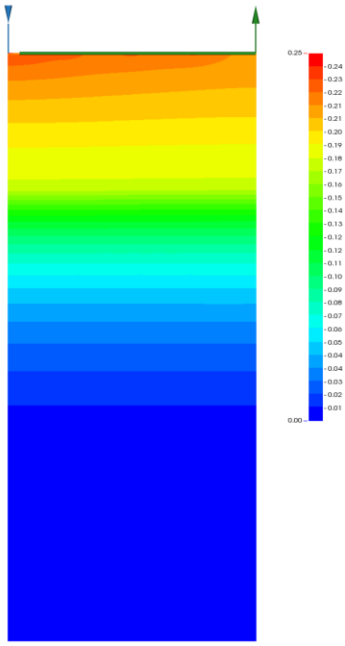

Figure 10: Gas saturation distribution within the core (simulation) after one day of start of CO_2 diffusion into the live oil.

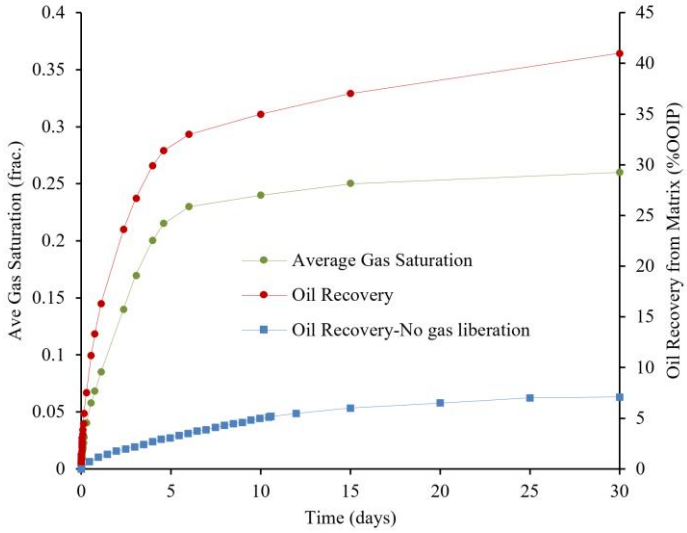

Figure 11: The oil recovery profiles generated from numerical simulations plotted against time for the two considered scenarios. In the presence of light hydrocarbon gas liberation, a significant increase in oil recovery took place as the oil phase was replaced with the liberated gas.

3.2.2 Large-scale numerical simulations

For the large-scale numerical simulations, a sector model (using the CMG-GEM compositional simulator) with two horizontal wells was used. Each horizontal well contained five planar fractures. The reservoir pressure and temperature were set to the tuned fluid model to accurately capture the gas liberation mechanism. The simulated sector was saturated with live oil. The initial pressure of the reservoir was set to 8000 psi. The well pressures were drawdown to the bubble point pressure of the oil, which prevents gas formation in the matrices during the primary pressure drawdown stage and hence, gas liberation due to CO_2 transfer can be identified. A series of 11 CO_2 huff-n-puff cycles were then performed, cycling the

pressure from the initial pressure (huff pressure) to the oil original bubble point pressure (puff pressure). Two simulations were performed; (i) using conventional parameters leading to no gas liberation and (ii) parameters from the tuned fluid model triggering in-situ gas liberation. Comparison of the results of these models can illustrate the importance of the gas liberation process and that neglecting this process can lead to significant under-estimation of CO_2 EOR and CO_2 storage efficiencies in shale and tight oil reservoirs.

The computation grid used for the sector numerical simulation is shown in Figure 12. The matrix properties are identical to that used in the laboratory-scale numerical simulations assuming a homogeneous reservoir. The fracture permeability was 50 mD and grid cells around the hydraulic fractures were refined into smaller sizes to provide better accuracy of the flow near the fractures. The sector numerical simulation was run for 10 years of simulation time under natural depletion with the wells operating under constant bottom hole pressure (equal to the bubble point pressure of the oil). Subsequently, the CO_2 injection was performed in a huff-n-puff mode with sequential cycles. In each cycle, CO_2 was injected to pressurize the wells up to the initial reservoir pressure and after a 2 month soaking period, the bottom hole pressure was dropped to the original bubble point pressure of the oil for drawdown periods.

The impact of the light hydrocarbon phase liberation was studied by comparing three simulations: (i) depletion for 30 years, (ii) 10 years of depletion followed by CO_2 huff-n-puff for 20 years with no gas liberation, and (iii) 10 years of depletion followed by CO_2 huff-n-puff for 20 years taking account of gas liberation. For each huff-n-puff cycle, the soaking period was 2 months followed by 22 months of pressure drawdown. Figure 13 shows the oil recovery profiles for these three cases. If the sector was operated under natural depletion, 9.9% of the original oil would be produced. If CO_2 EOR is considered with parameters accounting for gas liberation, the oil recovery from the sector can reach to 19.86%, which is 10% additional oil recovery. Therefore, in-situ gas liberation is the predominant mechanism controlling the performance of CO_2 scenarios in shale oil reservoirs. However, hen CO_2 huff-n-puff cycles were performed with parameters leading to no in-situ gas liberation, 4.2% additional oil recovery could be obtained. This amount of additional oil recovery is similar that found in previous studies[4,10] where the gas liberation was overlooked. Oil swelling and viscosity reduction are the major processes reported to have been behind the 4.2% of additional oil recovery. Another driving force for expelling oil out of the matrix, the expansion of CO_2 forced into the matrices due to pressurisation was overlooked. During pressurisation, when CO_2 was pumped into the fractures, CO_2 would invade the matrices and CO_2 expansion during the drawdown period could lead to some additional oil production. Recently, through laboratory experiments, the expansion of the gas in the vicinity of the fractures has been identified as an important mechanism in tight formations[31], which is in agreement with results reported in our numerical simulations.

In the third case, which takes account of the consequences of a liberated light hydrocarbon gas phase, the diffusion of CO_2 into this gas phase play a major role. The CO_2 diffusion coefficient in gas phase was set to 8×10^{-3} cm^2/s as suggested elsewhere[73]. To visualize the difference between results obtained in the simulations with and without in-situ gas liberation, a map of gas saturation distribution at end of huff-n-puff cycles are shown in Figure 14. The amount of gas saturation is significantly higher when in-situ gas liberation is taken into account. Notably, the simulation results demonstrate that CO_2 interaction with the live oil leads to gas liberation where CO_2 penetrates into the live oil.

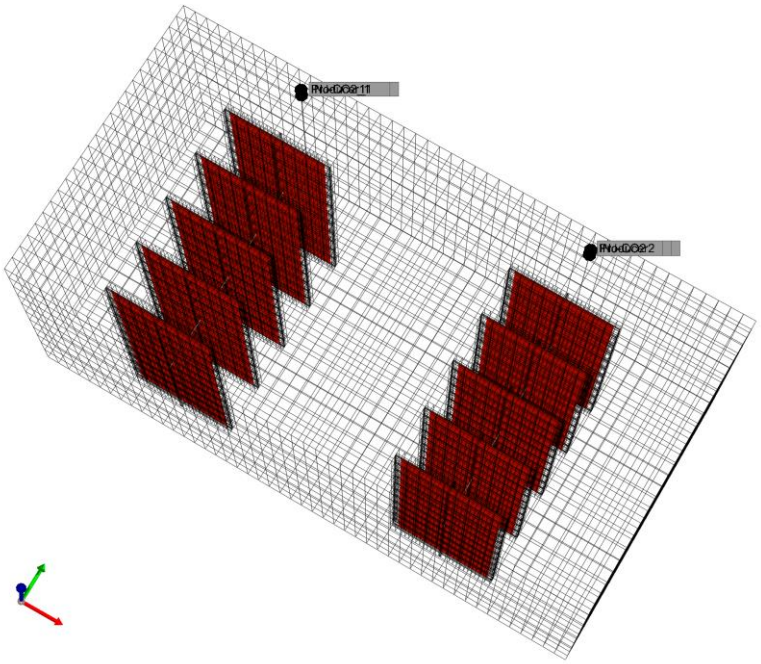

Figure 12: Field-scale (sector) model used for the numerical simulation of CO_2 EOR with two horizontal wells. The horizontal wells were fractured with five planar fractures. The rectangles in the model represent the fractures. The model was generally divided into 48 grids in x direction, 24 grids in y direction, and 11 grids in z direction. Each grid block has dimension of 50×50 ft in x and y and 20 ft in z. The model is then refined around the hydraulic fractures where grid blocks hosting the perforations are further divided into 5×7×1 sub-grids. The indicator on the left side of the image shows red, green, and blue arrows for x,y, and z direction, respectively. Matrix and fracture permeability were 0.001 and 50 mD, respectively.

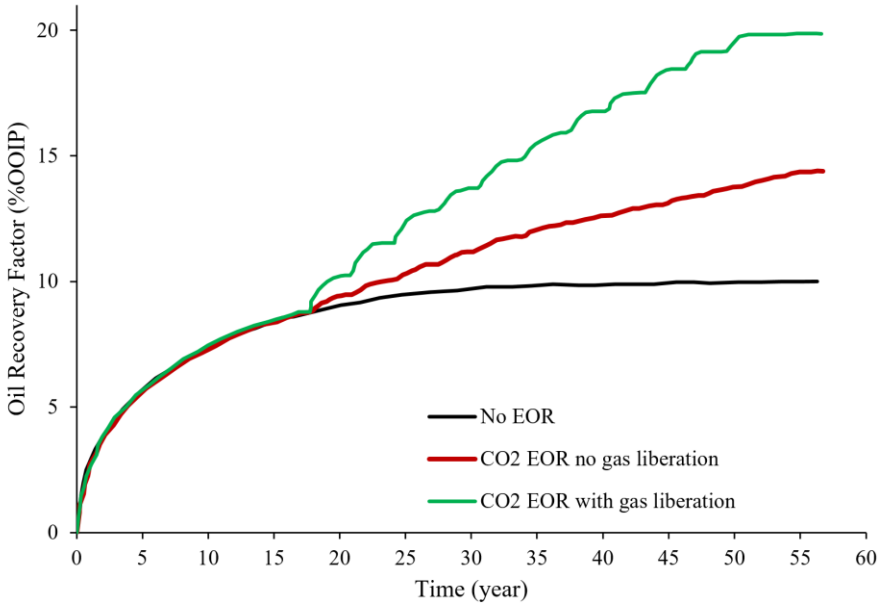

Figure 13: Cumulative oil recovery (in percent of original oil in place) profiles for natural depletion (in black), CO_2 EOR with no gas liberation (in red), and CO_2 EOR with gas liberation (in green). Significant additional oil recovery can be achieved by CO_2 huff-n-puff if the EOS parameters are modified to capture the gas liberation.

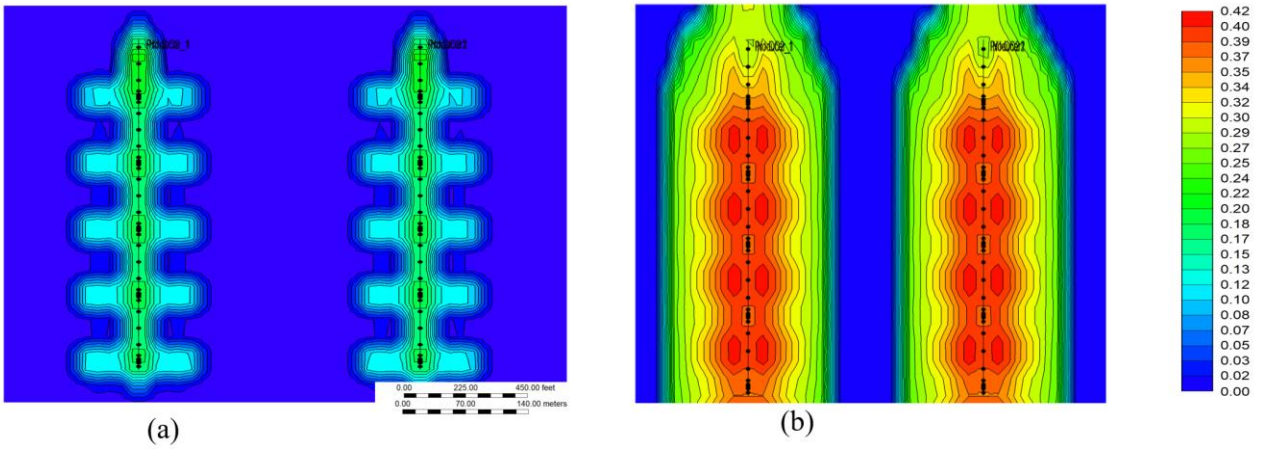

Figure 14: Gas saturation distribution at the end of CO_2 huff-n-puff for two cases: (a) with no gas liberation mechanism (left hand side image) and (b) with modified parameters to capture gas liberation (right hand side image). Significant amount of gas saturation was formed in the vicinity of the horizontal wells leading to significant additional oil recovery and CO_2 storage capacity.

3.2.3. CO_2 storage

In addition to the additional oil recovery, liquid-rich shale formations can be considered for CO_2 storage using CO_2 huff-n-puff. As numerous wells have been drilled for shale oil production, the synergy between enhanced oil recovery and CO_2 storage is evident. The simulation results presented in Figure 14 indicate that a substantial amount of gas was formed in the shale sector model. Provided that the in-situ liberated gas contained 75% of CO_2 (under pressure and temperature), an enhanced CO_2 capillary storage capacity was attained due to gas phase creation. This additional CO_2 storage would be in addition to the CO_2 dissolved in the liquid oil phase. Based on the numerical simulation results performed assuming no gas was liberated, only 9.1% of the total injected CO_2 was stored by its dissolution to the liquid oil phase after

all huff-n-puff cycles. When gas liberation was taken into account, 26.9% of the injected CO_2 was stored, an increase of nearly a factor of 3. The enhanced CO_2 storage capacity was achieved by the transfer of CO_2 into the gas phase and through the improved CO_2 diffusion through the liberated gas phase.

In terms of CO_2 storage capacity, the liberated gas can have a similar storage capacity as the oil. During the early huff-n-puff cycles, the CO_2 dissolved into the liberated gas phase would be produced back up the well whereas, after the third cycle, the simulation results demonstrate the significant increase in CO_2 storage in the liberated gas due to diffusive penetration. To analyse the performance of CO_2 huff-n-puff for CO_2 storage purposes, Figure 15a compares the cumulative ratio of remaining CO_2 to that injected into the formation $\left(\frac{remained\ CO2}{injected\ CO2}\right)$. Figure 15b also shows the sequential ratio of the injected CO_2 storage during consecutive huff-n-puff cycles. The $\left(\frac{remained\ CO2}{injected\ CO2}\right)$ ratio during each cycle increases, attributable to the penetration of CO_2 via diffusion away from the fracture. During the early cycles the storage capacity due to CO_2 dissolution into the oil is higher than that of the gas phase due to CO_2 flow-back from the matrices surrounding the fractures. During the later cycles, however, the $\left(\frac{remained\ CO2}{injected\ CO2}\right)$ ratio increases such that carbon storage in the liberated gas eventually dominates over that dissolved in the oil. This results from the immobility of the CO_2 dissolved into the liberated gas phase. Figure 15b shows that, the first cycle is most the effective for carbon storage due to CO_2 penetration into the oil phase. Over time, however, the bulk of the carbon storage is due to its dissolution into the gas phase. This result stems from the relative quantity of methane and CO_2 in the liberated gas; as demonstrated in laboratory experiments[41]. During the early stage of gas liberation, methane dominates whereas during in later stages, CO_2 dominates. Another factor contributing to carbon storage is the transport of pressurised CO_2 into the shale formation during puff period. Pressurised CO_2 transport is limited to the rock surrounding the fractures and hence, most of this pumped CO_2 would be produced during the production period of huff-n-puff cycles.

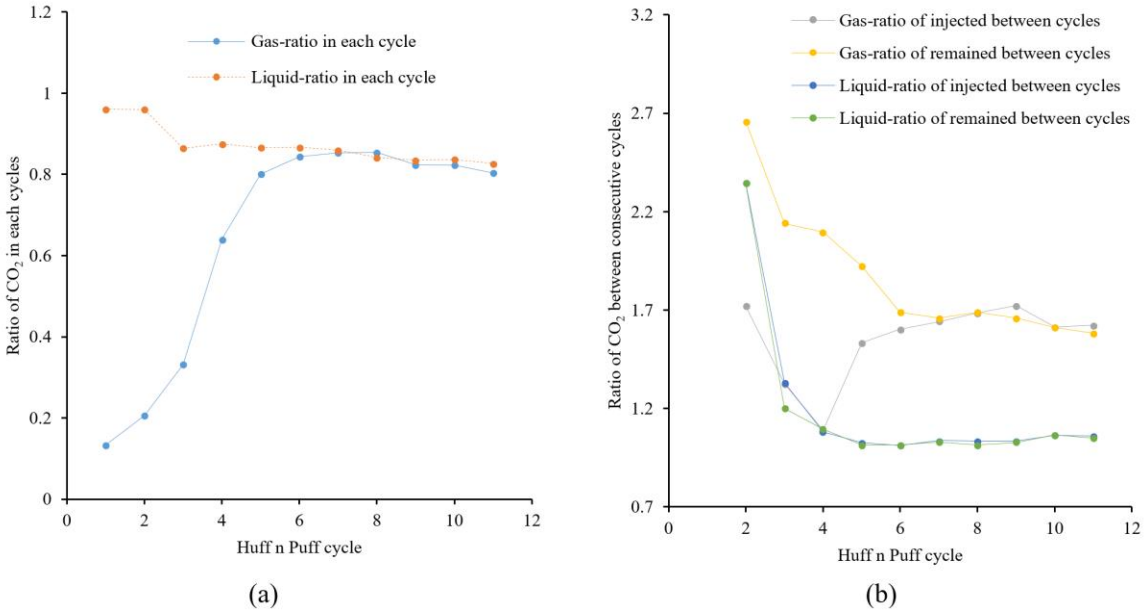

Figure 15: (a) Ratio of the remained divided by pumped CO_2 in each huff-n-puff cycle. For the liquid phase (orange curve), the dissolution of CO_2 in liquid oil phase is the dominant storage mechanism. When the wells were put in production mode, a significant quantity of CO_2 is stored in the oil. In the gas phase (blue curve), during the early cycles, the efficiency of CO_2 storage is poor due to flow back to the surface of injected CO_2. After the 4th cycle, efficiency of CO_2 storage for the gas phase is similar to that of the resident oil. (b) Ratio of the penetrated CO_2 during injection and production periods between consecutive cycles. The behaviour of liquid phase is different from gas phase.

Based on equivalent CO_2 emission of different fuels, one barrel of light crude oils (if burnt) emits approximately 325 kg of CO_2[74]. If it is assumed that the consumption of the oil would lead to this level of CO_2 emission, based on the sector model, the additional oil produced from CO_2 huff-n-puff process is half carbon-free, i.e. half of the equivalent emitted CO_2 from the produced oil is stored in the shale. The overall carbon storage efficiency of huff-n-puff process in the shale formation is 49.6% (49.6 percent of the emitted CO_2 by produced additional oil is stored). This calculation was done by dividing the remaining total CO_2 (as dissolved in oil and associated with the liberated gas) in the sector model after 10 huff-n-puff cycles by the equivalent emitted CO_2 of the additional oil produced over the 10 cycles. Thus, the injected and produced CO_2 quantitates during huff-n-puff process were not considered in the calculations.

The utilisation factor can be defined as the amount of CO_2 used to produce one barrel of oil[74]. The utilisation factor ($\frac{Injected\ CO_2\ in\ MSCF}{Produced\ oil\ in\ bbl}$) for the CO_2 injection process is 6.2, which is lower than that the corresponding average value of CO_2 displacement in conventional reservoirs[75]. Note that the implementation of CO_2 storage via its injection into liquid-rich shale formations does not require pure CO_2. It has been demonstrated by numerical simulations that the efficiency of pure CO_2 huff-n-puff in shale oils can be similar to a 90% pure CO_2 stream[19]. This behaviour can be attributed to diffusive transport of CO_2 and higher diffusion coefficient of CO_2 compared to methane and nitrogen.

The results of this study suggest that the conventional approaches to analyse the performance of CO_2 EOR in shale oils may be misleading. Althoughs this work is based on the analogy inferred from CO_2 and

carbonated water injection, it is likely that this mechanism would occur in shale oil rocks due to analogous diffusive based transport mechanism. This modelling attempt can highlight the importance of the process, which may lead to efforts to capture this process in the laboratory experiments. The in-situ gas liberation mechanism coupled to CO_2 diffusion can boost the reservoir energy pushing more oil out of the matrices. To accurately model the effects and consequences of in-situ gas liberation, a modified set of EOS parameters should be used, which account for the expulsion of light hydrocarbon components as CO_2 diffuses into live oils. Therefore, conventional hydrocarbon extraction by CO_2 may need to be revisited for systems modelled based on the diffusive mass transfer of CO_2. Also, although saturating ultra-tight cores with live oils is cumbersome, it is essential to investigate CO_2 interactions with representative live oil under full reservoir conditions. Notably, laboratory experiments under reduced conditions may not be able to capture this gas liberation mechanism and thereby under-estimating CO_2 EOR efficiencies.

4. Conclusions

To demonstrate the importance of in-situ gas liberation during CO_2 injection in shale and tight oil reservoirs, a series of analytical solutions and numerical simulations were performed. Carbon dioxide diffusion into live oils triggers the liberation of light hydrocarbon components as a distinct gas phase. This liberation of this gaseous phase can increase the grid pressure by almost 250 psi (higher pressure increases in tighter formations). This pore-scale phenomenon leads to significant enhanced oil recovery and CO_2 storage in fractured formations. It was observed that significant additional oil recovery can be achieved due to the liberation of gas. The liberated gas has a high CO_2 composition (i.e. 75%), which enhances CO_2 capillary storage.

Field-scale numerical simulations suggest 9.3% additional oil recovery would be achieved by CO_2 huff-n-puff. Approximately half of this additional recovery stems from the gas liberation mechanism. High gas saturations were distributed around the wellbore indicating the significant role of liberated gas on the performance of CO_2 EOR. Also, the CO_2 storage capacity of the shale reservoir is increased markedly due to in-situ gas liberation. Notably the CO_2 storage capacity of a liquid-rich shale formation can be doubled. Also, the CO_2 storage capacity of the liberated gas phase would be similar to that dissolved in the oil, thereby having CO_2 emission of the additional recovered oil. In summary, the results of this study highlights the fact that, conventional approaches assuming dead crude oils may underestimate substantially the for CO_2 EOR and carbon storage in shale and tight oil reservoirs.

Acknowledgements

This work is part of the Science for Clean Energy (S4CE) European research consortium funded by European Union's Horizon 2020 research and innovation programme under grant agreement No 764810. We would like to thank Computer Modeling Group Ltd. (CMG) for providing simulation package. Also, we appreciate feedback and comments from reviewers.

References

[1] S. Joshi, "EOR: Next Frontier for Unconventional Oil," *Journal of Petroleum Technology*, vol. 66, no. 06, pp. 20-22, 2014.

[2] J. Sheng, "Critical review of field EOR projects in shale and tight reservoirs," *Journal of Petroleum Science and Engineering*, vol. 159, pp. 654-665, 2017.

[3] B. Jai, J. Tsau and R. Barati, "A review of the current progress of CO2 injection EOR and carbon storage in shale oil reservoirs," *Fuel*, vol. 236, pp. 404-427, 2019.

[4] P. Zuloaga-Molero, Y. Xu, K. Sepehrnoori and B. Li, "Simulation Study of CO2-EOR in Tight Oil Reservoirs with Complex Fracture Geometries," *Scientific Reports*, vol. 6, p. 33445, 2016.

[5] S. Rassenfoss, "Shale EOR Works, But Will It Make a Difference?," *Journal of Petroleum Technology*, vol. 69, no. 10, p. 01 October 2017, 2017.

[6] S. Rassenfoss, "In the Shale Business, It's Time for Another Revolution," *Journal of Petroleum Technology*, vol. 70, no. 9, p. 23 July 2018, 2018.

[7] A. Katiyar, P. D. Patil, N. Rohilla, P. Rozowski, J. Evans, T. Bozeman and Q. Nguyen, "Industry-first hydrocarbon-foam EOR pilot in an unconventional reservoir: design, implimentation, and performance analysis," in *Unconventional Resources Technology Conference*, Denver, Colorado, USA, 2019.

[8] F. Tuero, M. Crotti and I. Labayen, "Water Imbibition EOR Proposal for Shale Oil Scenarios," in *SPE Latin America and Caribbean Petroleum Engineering Conference, 17-19 May*, Buenos Aires, Argentina, 2017.

[9] F. Du and B. Nojabaei, "A Review of Gas Injection in Shale Reservoirs: Enhanced Oil/Gas Recovery Approaches and Greenhouse Gas Control," *Energies*, vol. 12, p. 2355, 2019.

[10] D. Alfarge, M. Wei and B. Bai, "Factors Affecting CO2-EOR in Shale-Oil Reservoirs: Numerical Simulation Study and Pilot Tests," *Energy and Fuels*, vol. 31, pp. 8462-8480, 2017.

[11] B. H. Todd, "Huff-N-Puff Gas Injection Pilot Projects in the Eagle Ford," Calgary, Alberta, Canada, 2018.

[12] B. H. Todd and J. Evans, "Improved Oil Recovery IOR Pilot Projects in the Bakken Formation," Denver, Colorado, USA, 2016.

[13] B. H. Todd and S. Shoaib, "CO2 Flooding to Increase Recovery for Unconventional Liquid-rich Reservoirs," *Journal of Energy Resources Technology*, vol. 136, pp. 022801-1 to 10, 2014.

[14] IPCC, " Global Warming of 1.5°C. An IPCC Special Report on the impacts of global warming of 1.5°C.," in Press, Intergovernmental Panel on Climate Change, 2018.

[15] J. M. Matter, M. Stute, S. O. Snæbjornsdottir, E. H. Oelkers, S. R. Gislason, E. S. Aradottir, B. Sigfusson, I. Gunnarsson, H. Sigurdardottir, E. Gunnlaugsson, G. Axelsson, H. A. Alfredsson, D. Wolff-Boenisch, K. Mesfin, D. F. Taya, J. Hall, K. Dideriksen and W. S. Broecker, "Rapid carbon mineralization for permanent disposal of anthropogenic carbon dioxide emissions," *Science*, vol. 352, no. 6291, pp. 1312-1314, 2016.

[16] S. R. Gislason and E. H. Oelkers, "Carbon storage in basalt," *Science*, vol. 344, no. 6182, pp. 373-374, 2014.

[17] V. Pranesh, "Subsurface CO2 storage estimation in Bakken tight oil and Eagle Ford shale gas condensate reservoirs by retention mechanism," *Fuel*, vol. 215, pp. 580-591, 2018.

[18] H. Pu, Y. Wang and Y. Li, "How CO2-Storage Mechanisms Are Different in Organic Shale: Characterization and Simulation Studies," *SPE Journal*, vol. 23, pp. 661-671, 2018.

[19] P. Mahzari, T. Mitchell, A. P. Jones and E. H. Oelkers, "A New Mechanism for Enhanced Oil Recovery by CO2 in Shale Oil Reservoirs," in *IOR 2019 – 20th European Symposium on Improved Oil Recovery*, Pau, France, 2019.

[20] P. Mahzari, E. H. Oelkers, T. Mitchell and A. P. Jones, "An Improved Understanding About CO2 EOR and CO2 Storage in Liquid-Rich Shale Reservoirs," in *SPE Europec featured at 81st EAGE Conference and Exhibition*, London, England, UK, 2019.

[21] B. Eftekhari, M. Mardar and T. W. Patzek, "Field data provide estimates of effective permeability, fracture spacing, welldrainage area and incremental production in gas shales," *Journal of Natural Gas Science and Engineering*, vol. 56, pp. 141-151, 2018.

[22] R. B. Jackson, A. Vengosh, J. W. Carey, R. J. Davies, T. H. Darrah, F. O'Sullivan and G. Petron, "The environmental costs and benefits of fracking," *Annual Review of Environment and Resources*, vol. 39, pp. 327-362, 2014.

[23] L. Lei, C. Wang, D. Li, J. Fu, Y. Su and Y. Lv, "Experimental investigation of shale oil recovery from Qianjiang core samples by the CO2 huff-n-puff EOR method," *RSC Advances*, vol. 9, pp. 28857-28869, 2019.

[24] T. Gamadi, J. Sheng, M. Soliman, H. Menouar, M. Watson and H. Emadbaladehi, "An Experimental Study of Cyclic CO2 Injection to Improve Shale Oil Recovery," in *SPE Improved Oil Recovery Symposium*, Tulsa, Oklahoma, USA,

2014.

[25] H. Wang, Z. Lun, C. Lv, D. Lang, B. Ji, M. Luo, W. Pan, R. Wang and K. Gong, "Measurement and Visualization of Tight Rock Exposed to CO2 Using NMR Relaxometry and MRI," *Scientific Reports,* vol. 7, p. 44354, 2017.

[26] J. J. Sheng, T. Cook, W. Barnes, F. Mody, M. Watson, M. Porter and H. Viswanathan, "Screening of the EOR Potential of a Wolfcamp Shale Oil Reservoir," in *49th U.S. Rock Mechanics/Geomechanics Symposium, 28 June-1 July*, San Francisco, California, 2015.

[27] C. Carpenter, "Laboratory Investigation Targets EOR Techniques for Organic-Rich Shales," *Journal of Petroleum Technology,* vol. 71, no. 07, pp. 69-71, 2019.

[28] L. Jin, S. Hawthorne, J. Sorensen, L. Pekot, B. Kurz, S. Smith, L. Heebink, V. Herdegen, N. Bosshart, J. Torres, C. Dalkhaa, K. Petereson, C. Gorecki, E. Steadman and J. Harju, "Advancing CO2enhanced oil recovery and storage in unconventional oilplay—Experimental studies on Bakken shales," *Applied Energy,* vol. 208, pp. 171-183, 2017.

[29] L. Jin, J. A. Sorenson, S. B. Hawthorne, S. A. Smith, L. J. Pekot, N. W. Bosshart, M. E. Burton-Kelly, D. J. Miller, C. B. Grabanski, C. D. Gorecki, E. N. Steadman and J. A. Harju, "Improving Oil Recovery by Use of Carbon Dioxide in the Bakken Unconventional System: A Laboratory Investigation," *SPE Reservoir Evaluation & Engineering,* vol. 20, no. 03, pp. 602-612, 2017.

[30] J. A. Sorensen, B. A. Kurz, S. B. Hawthrone, L. Jin, S. A. Smith and A. Azenkeng, "Laboratory characterization and modeling to examine CO2 storage and enhanced oil recovery in an unconventional tight oil formation," *Energy Procedia,* vol. 114, pp. 5460-5478, 2017.

[31] p. Nguyen, J. W. Carey, H. S. Viswanathan and M. Porter, "Effectiveness of supercritical-CO2and N2huff-and-puffmethods of enhancedoil recovery in shale fracture networks using microfluidic experiments," *Applied Energy,* vol. 230, pp. 160-174, 2018.

[32] T. Wan and H. Liu, "Exploitation of fractured shale oil resources by cyclic CO2 injection," *Petroleum Science,* vol. 15, pp. 552-563, 2018.

[33] E. Kerr, K. K. Venepalli, K. Patel, R. Ambrose and J. Erdle, "Use of Reservoir Simulation to Forecast Field EOR Response - An Eagle Ford Gas Injection Huff-N-Puff Application," in *SPE Hydraulic Fracturing Technology Conference and Exhibition, 4-6 February,* , The Woodlands, Texas, USA, 2020.

[34] A. Mansour, T. Gamadi, H. Emadibaladehi and M. Watson, "Limitation of EOR Applications in Tight Oil Formation," in *SPE Kuwait Oil & Gas Show and Conference, 15-18 October*, Kuwait City, Kuwait, 2017.

[35] M. S. Kanfar, S. M. Ghaderi, C. R. Clarkson, M. M. Reynolds and C. Hetherington, "A Modeling Study of EOR Potential for CO2 Huff-n-Puff in Tight Oil Reservoirs - Example from the Bakken Formation," in *SPE Unconventional Resources Conference, 15-16 February*, Calgary, Alberta, Canada, 2017.

[36] A. Al Mesmari, P. Mahzari and M. Sohrabi, "Modelling Formation of a New Fluid Phase During Carbonated Water Injection," Bangkok, Thailand, 2016.

[37] A. A. Zick, "A Combined Condensing/Vaporizing Mechanism in the Displacement of Oil by Enriched Gases," in *SPE Annual Technical Conference and Exhibition, 5-8 October*, New Orleans, Louisiana, 1986.

[38] B. Haghshenas, F. Qanbari and C. R. Clarkson, "Simulation of Enhanced Recovery using CO2 in a Liquid-Rich Western Canadian Unconventional Reservoir: Accounting for Reservoir Fluid Adsorption and Compositional Heterogeneity," in *SPE Unconventional Resources Conference, 15-16 February*, Calgary, Alberta, Canada, 2017.

[39] A. J. Claderon and N. J. Pekney, "Optimization of enhanced oil recovery operations in unconventional reservoirs," *Applied Energy,* vol. 258, p. 114072, 2020.

[40] P. Mahzari, P. Tsolis, M. Sohrabi, S. Enezi, A. A. Yousef and A. Eiden, "Carbonated water injection under reservoir conditions; in-situ WAG-type EOR," *Fuel,* vol. 217, pp. 282-296, 2018.

[41] M. Seyyedi, P. Mahzari and M. Sohrabi, "An integrated study of the dominant mechanism leading to improved oil recovery by carbonated water injection," *Journal of Industrial and Engineering Chemistry,* vol. 45, pp. 22-32, 2017.

[42] P. Mahzari, P. Tsolis, M. Sohrabi, S. Enezi, A. Yousef and A. Eiden, "Carbonated water injection under reservoir conditions; in-situ WAG-type EOR," *Fuel,* vol. 217, pp. 285-296, 2018.

[43] F. M. Orr, R. T. Johns and B. Dindoruk, "Development of Miscibility in Four-Component CO2 Floods," *SPE Reservoir Engineering,* vol. 8, no. 02, pp. 135-142, 1993.

[44] W. W. Monroe, M. K. Silva, L. L. Larson and F. M. Orr, "Composition Paths in Four-Component Systems: Effect of Dissolved Methane on 1D CO2 Flood Performance," *SPE Reservoir Engineering,* vol. 5, no. 03, pp. 423-432, 1990.

[45] Y. Wang and F. M. Orr, "Analytical calculation of minimum miscibility pressure," *Fluid Phase Equilibria,* vol. 139, pp. 101-124, 1997.

[46] J. E. Burger and K. K. Mohanty, "Mass Transfer From Bypassed Zones During Gas Injection," *SPE Reservoir Engineering,* vol. 12, no. 02, pp. 124-130, 1997.

[47] M. Ding, Y. Wang, Y. Han, M. Gao and R. Wang, "Interactions in bypassed oil-CO2systems and their utilization in enhancingthe recovery of bypassed oil," *Fuel,* vol. 237, pp. 1068-1078, 2019.

[48] D. Alfarge, M. Wei, B. Bai and A. Almansour, "Effect of Molecular-Diffusion Mechanisim on CO2 Huff-n-Puff Process in Shale-Oil Reservoirs," in *SPE Kingdom of Saudi Arabia Annual Technical Symposium and Exhibition, 24-27 April*, Dammam, Saudi Arabia, 2017.

[49] T. Wan, J. Sheng and M. Watson, "Compositional Modeling of the Diffusion Effect on EOR Process in Fractured Shale Oil Reservoirs by Gas Flooding," in *SPE/AAPG/SEG Unconventional Resources Technology Conference, 25-27 August*, Denver, Colorado, USA, 2014.

[50] B. Jia, J. Tsau and R. Barati, "Role of Molecular Diffusion in Heterogeneous Shale Reservoirs During CO2 Huff-n-puff," in *SPE Europec featured at 79th EAGE Conference and Exhibition, 12-15 June*, Paris, France, 2017.

[51] M. Seyyedi, P. Mahzari and M. Sohrabi, "A comparative study of oil compositional variations during CO2 and carbonated water injection scenarios for EOR," *Journal of Petroleum Science and Engineering,* vol. 164, pp. 685-695, 2018.

[52] M. Seyyedi, P. Mahzari and M. Sohrabi, "A Fundamental Micro Scale Study of the Roles of Associated Gas Content and Different Classes of Hydrocarbons on the Dominant Oil Recovery Mechanism by CWI," *Scientific Reports,* vol. 9, p. 5996, 2019.

[53] P. Mahzari, A. P. Jones and E. H. Oelkers, "An integrated evaluation of enhanced oil recovery and geochemical processes for carbonated water injection in carbonate rocks," *Journal of Petroleum Science and Engineering,* vol. 181, p. 106188, 2019.

[54] S. Fakher, "Investigating Factors that May Impact the Success of Carbon Dioxide Enhanced Oil Recovery in Shale Reservoirs," in *SPE Annual Technical Conference and Exhibition, 30 September - 2 October*, Calgary, Alberta, Canada, 2019.

[55] T. H. Kim, J. Cho and K. S. Lee, "Evaluation of CO2 injection in shale gas reservoirs with multi-component transport and geomechanical effects," *Applied Energy,* vol. 190, pp. 1195-1206, 2017.

[56] P. Mahzari, A. Al Mesmari and M. Sohrabi, "Co-history Matching: A Way Forward for Estimating Representative Saturation Functions," *Transport in Porous Media,* vol. 125, no. 3, pp. 483-501, 2018.

[57] J. A. Coutinho, G. M. Kontogeorgis and E. H. Stenby, "Binary Interaction parameters for nonpolar systems with cubic equation of state: a theoritical approach 1. CO2/hydrocarbons using SRK equation of state," *Fluid Phase Equilibria,* vol. 102, pp. 31-60, 1994.

[58] J. A. Coutinho, P. M. Vlamos and G. M. Kontogeorgis, "General Form of the Cross-Energy Parameter of Equations of State," *Ind Eng Chem Res,* vol. 39, pp. 3076-3082, 2000.

[59] D. Peng and D. Robinson, "A new Two-Constant Equation of State," *Ind Eng Chem Fundam,* vol. 15, pp. 50-64, 1976.

[60] M. S. Al-Kadem, A. S. Al-Mashhad, M. S. Al-Dabbous and A. S. Sultan, "Integrating Peng Robinson EOS With Association Term for Better Minimum Miscibility Pressure Estimation," in *SPE Kingdom of Saudi Arabia Annual Technical Symposium and Exhibition, 23-26 April*, Dammam, Saudi Arabia, 2018.

[61] J. H. Lee and K. S. Lee, "Investigation of asphaltene-derived formation damage and nano-confinement on the performance of CO2 huff-n-puff in shale oil reservoirs," *Journal of Petroleum Science and Engineering,* vol. 182, p. 106304, 2019.

[62] Z. Shen and J. J. Sheng, "Experimental and numerical study of permeability reduction caused by asphaltene precipitation and deposition during CO2 huff and puff injection in Eagle Ford shale," *Fuel,* vol. 211, pp. 432-445, 2018.

[63] B. Wei, X. Zhang, J. Liu, H. Xiang and X. Xu, "Supercritical CO2-EOR in an asphaltenic tight sandstone formation and the changes of rock petrophysical properties induced by asphaltene precipitation," *Journal of Petroleum Science and Engineering,* vol. 184, p. 106515, 2020.

[64] S. Wu, Z. Li and H. K. Sarma, "Influence of confinement effect on recovery mechanisms of CO2-enhancedtight-oil recovery process considering critical properties shift, capillarity and adsorptio," *Fuel,* vol. 262, p. 116569, 2020.

[65] K. Zhang, Q. Liu, S. Wang, D. Feng, K. Wu, X. Dong, S. Chen and Z. Chen, "Effects of Nanoscale Pore Confinement on CO2 Displacement," in *Unconventional Resources Technology Conference, 1-3 August*, San Antonio, Texas, 2016.

[66] G. Yang, Z. Fan and X. Li, "Determination of confined fluid phase behavior using extended Peng-Robinson equation of state," *Chemical Engineering Journal,* vol. 378, p. 122032, 2019.

[67] J. Hwang and R. Pini, "Supercritical CO2 and CH4 Uptake by Illite-Smectite Clay Minerals," *Environ. Sci. Technol.,* vol. 53, pp. 11588-11596, 2019.

[68] N. Bagalkot and A. A. Hamouda, "Diffusion coefficient of CO2 into light hydrocarbons and interfacial tension of carbonated water–hydrocarbon system," *Journal of Geophysics and Engineering,* vol. 15, pp. 2516-2529, 2018.

[69] H. Sheikha, A. K. Mehrotra and M. Pooladi-Darvish, "An inverse solution methodology for estimating the diffusion coefficient of gases in Athabasca bitumen from pressure-decay data," *Journal of Petroleum Science and Engineering*, vol. 53, pp. 189-202, 2006.

[70] L. Shen and Z. Chen, "Critical review of the impact of tortuosity on diffusion," *Chemical Engineering Science*, vol. 62, pp. 3748-3755, 2007.

[71] N. R. Backeberg, F. Lacoviello, M. Rittner, T. M. Mitchell, A. P. Jones, R. Day, J. Wheeler, P. R. Shearing, P. Vermeesch and A. Striolo, "Quantifying the anisotropy and tortuosity of permeable pathways in clay-rich mudstones using models based on X-ray tomography," *Scientific Reports*, vol. 7, p. 14838, 2017.

[72] B. Ghanbarian, A. G. Hunt, R. P. Ewing and M. Sahimi, "Tortuosity in Porous Media: A Critical Review," *Soil Science Society of America Journal*, vol. 77, pp. 1461-1477, 2012.

[73] C. M. Oldenburg, D. Law, Y. Gallo and S. White, "Mixing of CO2 and CH4 in gas reservoirs: code comparison studies," *Greenhouse Gas Control Technologies - 6th International Conference*, vol. 1, pp. 443-448, 2003.

[74] R. J. Stewart and S. Haszeldine, "Carbon Accounting for Carbon Dioxide Enhanced Oil Recovery. Scottish Carbon Capture and Storage," Scottish Carbon Capture and Storage, Edinburgh, 2014.

[75] M. Verma, "Three approaches for estimating recovery factors in carbon dioxide enhanced oil recovery," U.S. Geological Survey Scientific Investigations Report, Reston, Virginia, 2017.

[76] A. Katiyar, P. Patil, N. Rohilla, P. Rozowski, J. Evans, T. Bozeman and Q. Nguyen, "Industry-First Hydrocarbon-Foam EOR Pilot in an Unconventional Reservoir: Design, Implementation, and Performance Analysis," in *SPE/AAPG/SEG Unconventional Resources Technology Conference, 22-24 July*, Denver, Colorado, USA, 2019.

[77] H. Pu and Y. Li, "CO2 EOR Mechanisms in Bakken Shale Oil Reservoirs," in *Carbon Management Technology Conference, 17-19 November*, Sugar Land, Texas, 2015.